Designing of a Dexterous Hand and Performance Evaluation Based on Teleoperation

Shukun Huang*,[a] , Zhenyuan Zhang†,[a], Mingqi Chen*, Zhaoyang Wu*, Qiang Li*,[b], and Zhong Ming*
*College of Big Data and Internet, Shenzhen Technology University, Shenzhen, China
†Future Technology School, Shenzhen Technology University, Shenzhen, China
[b]Email: liqiang1@sztu.edu.cn

***Abstract*—We proposed to design and evaluate a dexterous robotic hand through teleoperation. We introduced a dexterous hand with four fully actuated fingers, providing 16 degrees of freedom. A motor independently controls each joint, ensuring precise and flexible movements. The design incorporates an innovative joint distribution structure, enhancing the hand's flexibility and grasping capabilities. To validate the effectiveness of the design, we conducted a series of real-world experiments where the robotic hand replicated natural finger movements based on human hand gestures. The results demonstrated that the hand pose retargeting method successfully translates human gestures into precise and functional robotic hand movements, highlighting its potential for various practical applications in robotics.**

***Keywords*—dexterous hands, kinematic analysis, robot design, teleoperation, hand pose retargeting**

I. Introduction

Dexterous hands are critical components in robotics, offering the versatility needed for tasks ranging from precise manipulation to handling objects of various sizes and shapes. In the past years, dexterous capability of robotic hand has been demonstrated either via control method [1] or recent popular data driven approach [2]. In order to support these control methods, the mechanical design of dexterous hands has predominantly drawn inspiration from human anatomy, aiming to replicate the intricate movements and dexterity of human hands. Traditional dexterous hands often face challenges due to their complex joint structures, particularly in achieving sufficient degrees of freedom (DOF) for realistic and functional movements. The metacarpophalangeal (MCP) joint, which requires two DOFs for both flexion/extension and abduction-adduction, remains a significant challenge in compact designs. Addressing these challenges, our dexterous hand incorporates innovative mechanical designs, including fully actuated joints and modularized components, leading to improved flexibility, greater grasping strength and reduced manufacturing costs through 3D printing. Based on our work [1], [3], [4], [5] in the early stage, we designed a high DOF dexterous hand, analyzed its kinematics criteria and demonstrated how advancements in both mechanical design and teleoperation systems contributed to creating a high-performance robotic hand capable of addressing the demands of modern applications.

In addition to mechanical advancements, the effective operation of dexterous hands relies heavily on robust teleoperation systems. Teleoperation bridges the gap between human intention and robotic execution, enabling intuitive control and feedback for complex tasks. Our system leverages advanced techniques in hand gesture recognition, human-robot interface design, and real-time control mechanisms to ensure seamless and natural interactions. By using tools such as MediaPipe [6] and FrankMocap [7] for accurate hand tracking, and employing a ROS-based communication system for real-time data exchange, we provided a comprehensive framework for retargeting human hand movements into precise dexterous hand actions. This integrated approach not only enhances usability but also expands the application potential of dexterous hands in fields such as telemedicine, industrial automation, and imitation learning.

Through this work, we aimed to demonstrate how advancements in both mechanical design and teleoperation systems contribute to creating a high-performance dexterous hand capable of addressing the demands of modern applications.

II. System overview

A. Design of the dexterous hand

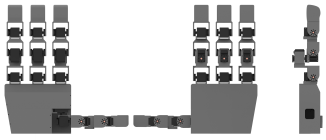

Fig. 1: Three views of our dexterous hand.

So far, the majority of dexterous hands have been created by imitating the anatomical structure of human hands. The fingers, excluding the thumb, are made up of three joints: the metacarpophalangeal joint (MCP), the proximal interphalangeal joint (PIP), and the distal interphalangeal joint (DIP). PIP and DIP are single-degree-of-freedom joints that allow flexion and extension. The MCP joint in the human hand is actually a spherical joint with certain limitations [8]. In dexterous hands, a spherical joint is almost impossible to implement, so in practice, the MCP joint is often regarded as a two-degree-of-freedom joint, which can achieve flexion and extension as well as abduction and adduction of the fingers. DIP and PIP are revolute joints, which are relatively easier to implement. Due to the use of a fully actuated design, the joint motors can only provide one degree of freedom in a single direction, making it difficult to achieve the two degrees of freedom of the MCP within such a small space. This greatly increases the complexity of the dexterous hand design and hinders the modularity of the fingers. It significantly

[a] First Author and Second Author contribute equally to this work.
[b] Qiang Li is the corresponding author.

increases the complexity of the dexterous hand design and hinders the modularization of the fingers. As shown in Fig 2-B, we referenced the mechanical implementation of the MCP joint from Leap-Hand [9]. By adding a link, we placed the two degrees of freedom of the MCP joint at the two ends of this additional link to avoid the intersection of the MCP joint axes. As depicted in Fig 2-A, this is the conventional joint layout adopted by most robotic hands, which we refer to as C-Hand. Research had shown that our adopted joint distribution structure offered superior flexibility compared to the alternative, as argued in IV-A1. Our dexterous hand has four fingers and adopts full drive design with 16 degrees of freedom (Shown in Fig 1). Each joint is independently controlled by a motor. The motors communicate and supply power through serial connection. All fingers, except for the thumb, are completely identical. Compared to the original design of the Leap-Hand, our hand is larger and has more powerful motor performance, and the 12 N\m maximum torque makes it more capable of grasping. At the same time, assembly costs are reduced by printing 3-D parts.

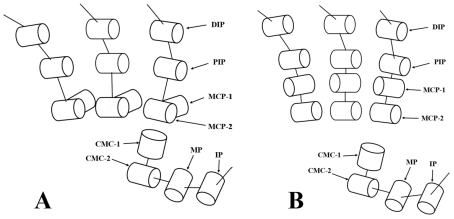

Fig. 2: **(A)** Joint distribution diagram of C-Hand [10], **(B)** Joint distribution diagram of Leap Hand

Table I presents the standard D-H parameter list using the Denavit-Hartenberg method [11] for the single finger of the mechanical arm modeling approach.

TABLE I: D-H parameter list of our dexterous hand's finger

i	θ_i	$d_i(mm)$	$a_i(mm)$	α_i (°)	offset (°)
1	0	17	0	$\pi/2$	0
2	q_2	0	47	-$\pi/2$	$\pi/2$
3	q_3	0	16	-$\pi/2$	0
4	q_4	0	52.13	0	0
5	q_5	0	70	0	0

The first link here is the distance of the first joint from the base. The thumb is the key to human dexterity, and the thumb of the dexterous hands is the key part that determines the grasping performance of the entire device [12]. Table II is the standard D-H parameter list for the thumb.

TABLE II: D-H parameter list of our dexterous hand's thumb

i	θ_i	$d_i(mm)$	$a_i(mm)$	α_i(°)	offset (°)
1	0	17	24.34	0	$\pi/2$
2	q_2	-36	0	-$\pi/2$	-$\pi/2$
3	q_3	46.12	0	$\pi/2$	$\pi/2$
4	q_4	0	60.51	0	$\pi/2$
5	q_5	0	63.37	0	0

B. Design of dexterous hand operating system

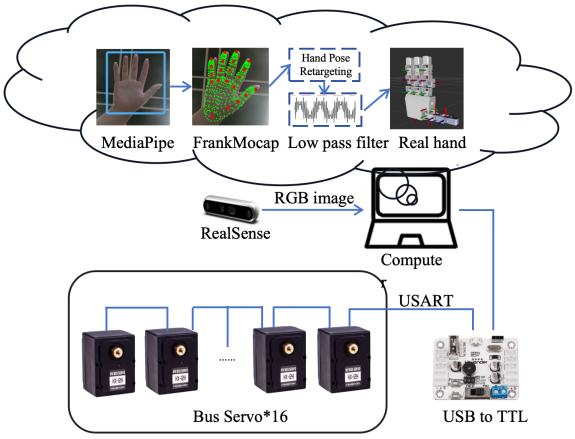

Fig. 3: Pipeline of a hand gesture control system: Using MediaPipe [6] and FrankMocap [7] for hand tracking, joint space mapping, and filtering to process movements, and controlling a robotic hand with servo motors through a computer via USART.

Our work aims to achieve robust dexterous hand control through human hand gestures. The pipeline of this strategy is shown in Fig 3, consisting of a hardware system and a software system, with communication handled via ROS for real-time control.

The hardware system comprises an Intel RealSense D455 for capturing RGB images, a computer for processing, and a bus servo motor system featuring 16 actuators. The RealSense D455 captures RGB images of the human hand, which are then processed by the computer to estimate hand pose and generate control angles. The processed joint angles are transmitted to the robotic hand via a USB-to-TTL interface using USART communication. All hardware components communicate through ROS topics, ensuring efficient and synchronized data transfer.

The software system involves hand pose estimation, hand pose retargeting, and jitter suppression. Our hand detection process starts with RGB frames, from which we extract and hand pose, along with shape parameters using MediaPipe [6] and FrankMocap [7]. MediaPipe tracks and crops the hand region, and Frankmocap takes the cropped image as input and regresses the shape and pose parameters of the human hand, even when self-occlusion occurs. We represent the hand using the SMPL-X [13] model to reconstruct a 3D hand model with shape and pose parameters. The pose data is retargeted into joint angles suitable for robotic hand actuators, and a low-pass filter ensures smooth motion by reducing noise.

III. Hand Pose Retargeting

Fig 2-B illustrates the degrees of freedom (DOF) of each finger in various robotic models. To adapt the human hand demonstration for a specific robot, a process known as hand pose retargeting is required. This involves computing the sequence of robot joint angles q_t^R at each time step t from a given sequence of human hand poses q_t^H obtained in previous process steps. We formulated this as an optimization problem:

$$\min_{q_t^R} \sum_{i=0}^{N} \|\alpha f_i^H(q_t^H) - f_i^R(q_t^R)\|^2 + \beta \|q_t^R - q_{t-1}^R\|^2 \quad (1)$$
$$\text{s.t.} \quad q_{\text{l}}^R \leq q_t^R \leq q_{\text{u}}^R,$$

The forward kinematics function for the human hand, denoted as $f_i^H(q_t^H)$, computes the i-th Task Space Vector (TSV) for the human hand, while the robot forward kinematics function, $f_i^R(q_t^R)$, calculates the corresponding TSV for the robot. A scaling factor, α, is introduced to account for variations in hand size between the human and dexterous hands. The parameters q_{l}^R and q_{u}^R define the lower and upper bounds, respectively, for the robot's joint positions.

The primary objective of the first term in the cost function is to identify the optimal joint configuration q_t^R, ensuring the alignment of the fingertip-palm and fingertip-phalanx TSVs for both the human and robot hands. In addition, to promote temporal consistency, a penalty term based on L2 normalization with a weight factor β is incorporated. This term discourages abrupt changes in joint positions, with the robot's joint configuration at time t, denoted as q_t^R, being initialized from the previous time step q_{t-1}^R. Simultaneously, human hand poses, represented by q_t^H, undergo preprocessing through a low-pass filter to reduce noise.

For the optimization process, Sequential Least-Squares Quadratic Programming in the NLopt [14] framework is utilized. In our implementation, the value of the scaling factor α is set to 8×10^{-3}. For more details, please refer to [15].

IV. Result and Discussion

A. Kinematic Analysis of Dexterous Hand

Kinematic analysis is a key process in robot development and is crucial for evaluating the performance of our dexterous hand. In this chapter, we analyzed the reachable workspace of the hand using the Matlab Robot Toolbox (RTB) and obtained the workspace volume of the single finger and the thumb using the envelope method. Finally, we calculated the structural length index (SLI) as an indicator for subsequent optimization of the dexterous hand.

1) Workspace analysis: The workspace of a robot refers to the set of all possible positions that the end-effector reference point can reach during all possible movements, which is determined by the geometric shape of the manipulator and the limits of joint motion. It is an important kinematic indicator for measuring the working capacity of a robot [16]. Currently, there are three main methods for determining the workspace of a robot: geometric methods, analytical methods, and numerical methods [17]. Among these, numerical methods offer a simple solution process and apply to any form of robotic structure, making them the most widely used. It is necessary to limit the angle of joint motion to calculate the reachable workspace. The limits of the single finger and the thumb joints are shown in Table III.

Using the Monte Carlo method in Matlab RTB to establish the spatial cloud map for the entire dexterous hand, the single finger, and C-Hand's finger (Shown in Fig 4).

TABLE III: Single finger, thumb, and C-Hand's finger joints limits range

	Finger	Thumb	C-Hand
q_1	[0,0]	[0,0]	[0,0]
q_2	[-10,100]	[0,90]	[-90,90]
q_3	[-90,90]	[-10,100]	[-10,100]
q_4	[-10,100]	[-10,100]	[-10,100]
q_5	[-10,100]	[-10,100]	[-10,100]

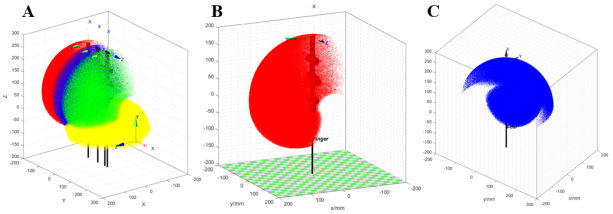

Fig. 4: **(A)** The workspace point cloud map of the entire hand, **(B)** The workspace point cloud map of the single finger, **(C)** The workspace point cloud map of C-Hand's finger.

Connecting adjacent points in the point cloud generates an envelope diagram of the workspace, which can be used to roughly calculate the volume of the workspace (Shown in Fig 5). Workspace volume calculated: V_F = 11623cm^3, V_T = 6542.26cm^3.

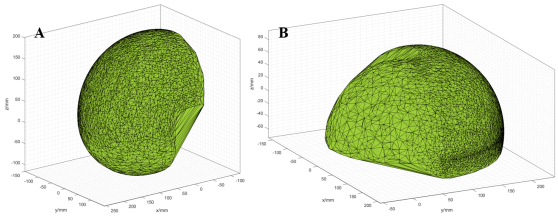

Fig. 5: **(A)** The workspace envelope of the single finger, **(B)** The workspace envelope of the thumb.

Comparing the workspace point clouds of the single and C-Hand's finger (Shown in Fig 4-B, C), it is observed that C-Hand's finger has a significant vacuum area on the plane where its MCP-1 is located. The boundary radius of this vacuum area is the sum of the lengths of the other links, and the tip cannot reach these areas. This is due to the angular limitation of MCP-1, which ranges from -90 to 90 degrees. To reach areas below the plane where the MCP-1 axis is located, it is necessary to reset the MCP-1 and then move the other joints, indicating that its motion space is not continuous. In contrast, the workspace point cloud of our dexterous hand's finger is a continuous curved surface, with no areas around it that the end effector cannot reach. The comparison revealed that the joint structure design of our dexterous hand's finger offered greater flexibility than that of the C-Hand.

2) Structural length index analysis: The structural length index (SLI) is one of many indicators to evaluate the performance of a manipulator. Its indicator reflects the structural efficiency of a robotic arm. In the design and optimization of robotic arms, the SLI helps to evaluate and compare the global performance of different design schemes, thereby selecting the optimal design parameters. It is defined as the ratio of the sum of the lengths of the robotic arm's links to the cube root of its end-effector reachable workspace volume [18], that is:

$$L = \sum_{i=1}^{n} a_i + d_i \tag{2}$$

$$Q_L = \frac{L}{\sqrt[3]{V}} \tag{3}$$

In Eq 2 and 3, V represents the workspace volume at the end of the manipulator, a_i and d_i are the link length and link bias, respectively. Bring V_F, V_T, a_i, and d_i for finger and thumb into it:

$$Finger : L_F = 20.213cm, Q_F = 0.8923$$

$$Thumb : L_T = 17.664cm, Q_T = 0.9445$$

In future work on design optimization, we will focus on reducing the value of SLI.

B. Real-World Robot Experiments

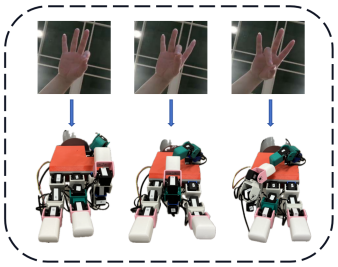

Fig. 6: Hand Gesture-Controlled robot experiment demonstration.

In real-world experiments, we assessed the system's ability to interpret hand gestures and translate them into precise movements of a dexterous robotic hand. The key predefined gestures tested included:

1) Index Finger Touching Thumb
2) Middle Finger Touching Thumb
3) Ring Finger Touching Thumb

C. Remarks and Discussion

The results showed the system reliably translated human gestures into precise robotic actions, with over 90% success across trials and robust gesture mapping.

Occasional ambiguities caused a 5-8% error rate, meaning the need for improved recognition. Nonetheless, the experiments validated the system's effectiveness in bridging human intention and robotic execution for versatile dexterous hand control.

V. Conclusion and Future Work

We proposed a robotic system that combines a dexterous, cost-effective dexterous hand with an intuitive teleoperation interface using an optimization method for retargeting. The system enabled precise and reliable grasping through advanced mechanical design and real-time gesture recognition, providing seamless human-robot interaction.

Future work will aim to enhance the dexterity of finger movements, the system's adaptability, gesture recognition accuracy, and the utilization of teleoperation data for imitation learning and reinforcement learning.

Acknowledgment

This work was supported by 2024 National Undergraduate Training Program for Innovation and Entrepreneurship of SZTU (S202414655019), and " Natural Science Foundation of Top Talent of SZTU".

References

[1] Q. Li, R. Haschke, B. Bolder, and H. Ritter, "Grasp point optimization by online exploration of unknown object surface," in *2012 12th IEEE-RAS International Conference on Humanoid Robots (Humanoids 2012)*. IEEE, 2012, pp. 417–422.

[2] O. M. Andrychowicz, B. Baker, M. Chociej, R. Jozefowicz, B. McGrew, J. Pachocki, A. Petron, M. Plappert, G. Powell, A. Ray *et al.*, "Learning dexterous in-hand manipulation," *The International Journal of Robotics Research*, vol. 39, no. 1, pp. 3–20, 2020.

[3] M. Chen, S. Li, F. Shuang, X. Liu, K. Luo, and W. He, "Lightweight 3d hand pose estimation by cascading cnns with reinforcement learning," *Pattern Recognition Letters*, vol. 174, pp. 137–144, 2023.

[4] C. Zeng, S. Li, Y. Jiang, Q. Li, Z. Chen, C. Yang, and J. Zhang, "Learning compliant grasping and manipulation by teleoperation with adaptive force control," in *2021 IEEE/RSJ International Conference on Intelligent Robots and Systems (IROS)*. IEEE, 2021, pp. 717–724.

[5] Q. Li, M. Meier, R. Haschke, H. Ritter, and B. Bolder, "Rotary object dexterous manipulation in hand: a feedback-based method," *International Journal of Mechatronics and Automation*, vol. 3, no. 1, pp. 36–47, 2013.

[6] C. Lugaresi, J. Tang, H. Nash, C. McClanahan, E. Uboweja, M. Hays, F. Zhang, C. Chang, M. Yong, J. Lee, W.-T. Chang, H. Wang, M. Georg, and M. Grundmann, "Mediapipe: A framework for building perception pipelines," *Cornell University - arXiv,Cornell University - arXiv*, Jun 2019.

[7] Y. Rong, T. Shiratori, and H. Joo, "Frankmocap: A monocular 3d whole-body pose estimation system via regression and integration," in *2021 IEEE/CVF International Conference on Computer Vision Workshops (ICCVW)*, Oct 2021. [Online]. Available: http://dx.doi.org/10.1109/iccvw54120.2021.00201

[8] J. Yu, X. Liu, and X. Ding, *Mathematic Foundation of Mechanisms and Robotics(Chinese version)*. China Machine Press, 2016. [Online]. Available: https://books.google.com.sg/books?id=masotAEACAAJ

[9] K. Shaw, A. Agarwal, and D. Pathak, "Leap hand: Low-cost, efficient, and anthropomorphic hand for robot learning," *arXiv preprint arXiv:2309.06440*, 2023.

[10] D.-H. Lee, J.-H. Park, S.-W. Park, M.-H. Baeg, and J.-H. Bae, "Kitech-hand: A highly dexterous and modularized robotic hand," *IEEE/ASME Transactions on Mechatronics*, vol. 22, no. 2, pp. 876–887, 2016.

[11] J. Denavit and R. S. Hartenberg, "A kinematic notation for lower-pair mechanisms based on matrices," 1955.

[12] H. Wang, S. Fan, and H. Liu, "An anthropomorphic design guideline for the thumb of the dexterous hand," in *2012 IEEE International Conference on Mechatronics and Automation*. IEEE, 2012, pp. 777–782.

[13] G. Pavlakos, V. Choutas, N. Ghorbani, T. Bolkart, A. A. A. Osman, D. Tzionas, and M. J. Black, "Expressive body capture: 3D hands, face, and body from a single image," in *Proceedings IEEE Conf. on Computer Vision and Pattern Recognition (CVPR)*, 2019, pp. 10 975–10 985.

[14] S. G. Johnson *et al.*, "The nlopt nonlinear-optimization package," 2014.

[15] Y. Qin, Y.-H. Wu, S. Liu, H. Jiang, R. Yang, Y. Fu, and X. Wang, *DexMV: Imitation Learning for Dexterous Manipulation from Human Videos*, Jan 2022, p. 570–587. [Online]. Available: http://dx.doi.org/10.1007/978-3-031-19842-7_33

[16] B. Siciliano, O. Khatib, and T. Kröger, *Springer handbook of robotics*. Springer, 2008, vol. 200.

[17] J.-P. Merlet, *Parallel robots*. Springer Science & Business Media, 2006, vol. 128.

[18] S. Patel and T. Sobh, "Manipulator performance measures-a comprehensive literature survey," *Journal of Intelligent & Robotic Systems*, vol. 77, pp. 547–570, 2015.